OL Organic Letters

pubs.acs.org/OrgLett Letter

C- and S-Shaped Perylene Diimide Heterohelicenes: Modular Synthesis and Spiral-Stair-Like π-Stacking

Li Zhang, Shuqi Chen, Jianbao Jiang, Xue Dong, Yapeng Cai, Hui-Jun Zhang, Jianbin Lin,* and Yun-Bao Jiang

Cite This: *Org. Lett.* 2022, 24, 3179–3183 Read Online

ACCESS | Metrics & More | Article Recommendations | Supporting Information

ABSTRACT: A number of *C*- and *S*-shaped perylene diimide (PDI) heterohelicenes with high dipole moments were synthesized from simple perylene tetrabutylester (PTE). Taking advantage of the weak coordination ability of the sterically crowded peri ester groups in PTE, efficient Rh(III)-catalyzed 2,8- and 2,11-bisiodinations of the perylene core were realized. The 2,8- and 2,11-diiodinated PTEs and PDIs represent key synthons for further *ortho*-π-extensions. In contrast to most helical π-skeletons that feature loose molecular packings, enantiomerically pure *C*-shaped PDI azahelicenes adopt unique spiral-stair-like π-stacking superstructures.

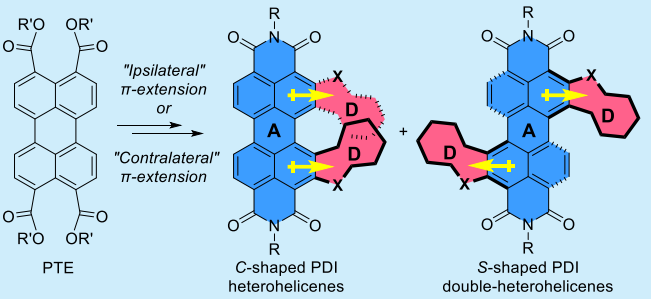

Helical π-systems, such as helicenes and their derivatives, that possess superb chiroptical properties and conjugated molecular orbitals are among the most promising candidates for chiral organic semiconductors.[1] On the other hand, with efficient exciton diffusion and charge transport, the one-dimensional (1D) π-stacking structures of π-conjugated molecules represent prime candidate building blocks for device miniaturization in various electronic and optoelectronic applications.[2] However, most screw-shaped distorted π-skeletons, especially the enantiomerically pure ones, can only adopt a loose molecular packing in the solid state.[3,4] This kind of dilemma is also encountered in other π-systems with large steric hindrance[5] or charge repulsion.[6]

To boost the electrical performance of helical π-systems while maintaining the high circular polarization selectivities, we recently described a skeleton-merging approach toward *ortho*-π-extended perylene diimide (PDI) double-[7] heterohelicenes through the distortion of the PDI core (acceptor, A) with four fused indoles or benzothiophenes (donor, D).[7,8] The PDI double helicenes (**I**, Scheme 1a) can thus inherit a high dissymmetry factor from the helical skeleton while maintaining an adequate level of the charge transport property. Compared to these symmetric fused D−A systems, their asymmetric fused counterparts, such as *C*- and *S*-shaped π-extended PDI heterohelicenes (**II** and **III**, respectively, Scheme 1b), can be characterized by large dipoles. The distribution of their molecular orbitals and crystal packing might be effectively tuned by strong dipole−dipole interactions in combination with other noncovalent interactions, leading to high carrier mobilities.[9] With this consideration, we herein report an efficient synthetic route for selective "ipsilateral (*C*-shaped)" and "contralateral (*S*-shaped)" π-extensions of the PDI core

Scheme 1. Three Different Types of *ortho*-π-Extended PDI Heterohelicenes and Theoretical Dipole Moments

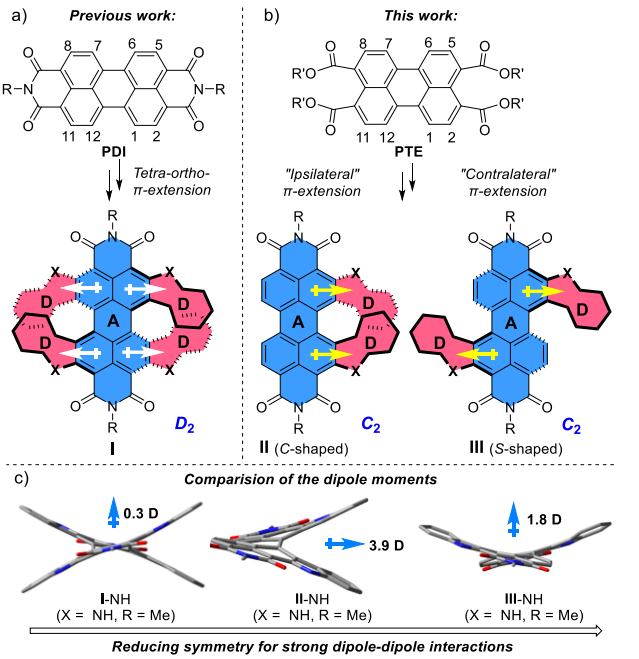

Received: March 16, 2022
Published: April 27, 2022

https://doi.org/10.1021/acs.orglett.2c00928
Org. Lett. 2022, 24, 3179−3183

starting from simple perylene tetrabutylester (PTE). The involvement of distinct heteroatoms (N, O, and S) finely tunes the absorption profiles and energy levels of the newly formed *C*- and *S*-shaped PDI heterohelicenes. Moreover, unlike the proposed arrangements of planar π-skeletons in most face-to-face $\pi-\pi$ stacked helical columns (Scheme 2a), enantiomerically pure *C*-shaped PDI heterohelicenes assembled into unique spiral-stair-like π-stacking structures through the interplay of steric repulsion, $\pi-\pi$ stacking, and dipolar interactions (Scheme 2b).

Scheme 2. Dispositions of π-Skeletons in (a) Face-to-Face and (b) Spiral-Stair-Like $\pi-\pi$ Stacked Helical Columns

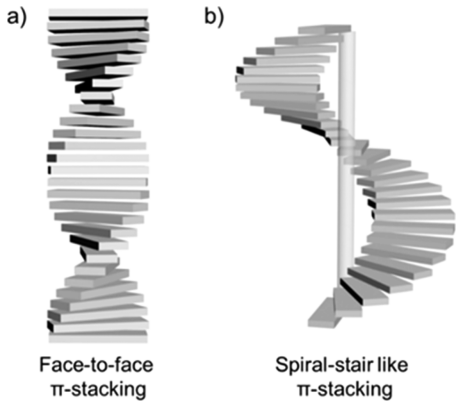

Initially, we evaluated the dipole moments of a series of indole-fused helical π-systems **I**-NH, **II**-NH, and **III**-NH (Scheme 1c) by performing DFT calculations using B3LYP/6-31G(d) method. *C*-Shaped **II**-NH and *S*-shaped **III**-NH exhibit much higher dipole moments (3.9 D for **II**-NH and 1.8 D for **III**-NH) than tetraindole-fused PDI **I**-NH (0.3 D), which confirmed the large dipoles of asymmetric fused D−A conjugated skeletons systems.

Encouraged by this result, we planned to synthesize **II** and **III** from 2,11- and 2,8-diiodinated PDI derivatives, respectively, via *ortho*-π-extensions.[7] Based on our recent developed efficient Rh(III)-catalyzed *ortho*-C−H iodination of PDIs, a mixture of 2,5-, 2,8-, and 2,11-diiodinated PDI derivatives could be produced in moderate yields.[10] It is, however, well-known that the isolation of these kinds of isomers is rather difficult, if not impossible, due to their similar polarities, especially on a relatively large scale.[11] Compared with imide carbonyls in PDIs,[12] the neighboring *peri*-ester substituents in PTE are more sterically crowded, which favors selective 2,8- and 2,11-bisiodination on the perylene core.[13] More than that, PTE is much more soluble than PDIs and thus might favor the following transformations. However, the ester group is more weakly directing than amide groups,[14] which might make the development of such protocols difficult. To our delight, our Rh(III)-catalyzed *ortho*-C−H iodination strategy is also applicable to PTE. The reaction of PTE (**1**) with *N*-iodosuccinimide (NIS) in the presence of 5 mol % $[Cp^*RhCl_2]_2$, 50 mol % $AgSbF_6$, and 1.1 equiv of $Cu(OAc)_2{\cdot}H_2O$ in 1,1,2,2-tetrachloroethane (TCE) at 80 °C for 16 h led to the selective formation of two diiodinated PTEs as a mixture in a 47% yield (Scheme 3 and Table S1). Small amounts of pure **2** and **3** were isolated for structural characterizations. The structure of 2,11-diiodinated PTE **3** was verified by ^{1}H NMR spectroscopy and a 1D NOE experiment (Figure S1). The structure of less polar 2,8-diiodinated PTE **2** was determined by both ^{1}H NMR spectroscopy (Figure S2) and single-crystal X-ray diffraction analysis (CCDC 2082691 and Figure S3). The ratio of **2** to **3** (3:2) was calculated from ^{1}H NMR spectra of the mixture (Figure S4). Notably, a novel $[Cp^{Et4Ph}RhI_2]_2$ complex featuring a sterically crowded Cp^{Et4Ph} ligand is more robust for these transformations, allowing the formation of **2** and **3** in an 80% yield. The gram-scale reaction (PTE, 5.0 mmol, 3.3 g) also worked smoothly in the presence of this new precatalyst and afforded the desired products in a 63% yield (2.9 g).

Scheme 3. Selective Double *ortho*-C−H Iodinations of PTE

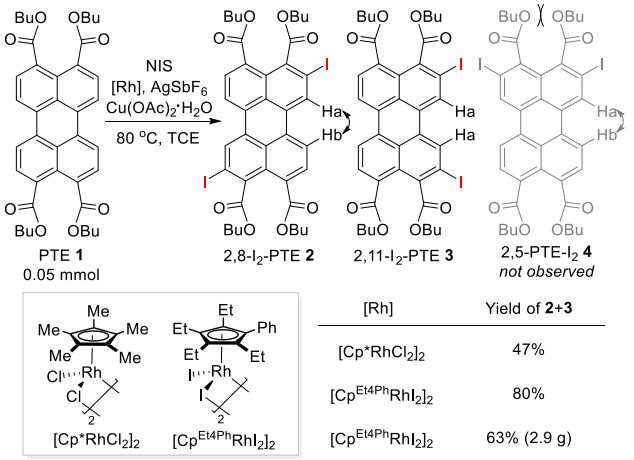

Then, the asymmetric fused PDI heterohelicenes were constructed from the diiodinated PTEs through two different approaches (Scheme 4). Treating mixture of **2** and **3** with chlorosulfonic acid at room temperature for 4 h afforded a mixture of diiodo-perylene dianhydrides (diiodo-PDAs) **5** and **6** in a 99% yield (Scheme 4a). The direct condensation of the diiodo-PDA mixtures with 2-octyldodecylamine produced 2,8-I_2-PDI **7** and 2,11-I_2-PDI **8**. They were separable from each other and were isolated in 50% and 54% yields, respectively. Starting from **7** and **8**, *S*-shaped PDI double-hetero[5]-helicenes **10a−c** and *C*-shaped PDI hetero[7]helicenes **12a−c** were synthesized through regioselective π-extensions (Scheme 4b and c, respectively). These "contralateral" and "ipsilateral" π-extension methods are not contingent on the PDI skeletons. As shown in Scheme 4d, *S*-shaped PDI double-azahelicenes **10d** and **10e** and *C*-shaped PDI azahelicenes **12d** and **12e** were readily produced from a mixture of diiodo-PTEs **2** and **3** through direct regioselective π-extensions, followed by hydrolysis and condensation. It is not necessary to separate the corresponding isomeric products for each reaction step before the last condensation.

The series of new PDI heterohelicenes all exhibited good solubilities in common organic solvents, such as CH_2Cl_2, $CHCl_3$, THF, and toluene. Their helical structures were confirmed by single-crystal X-ray crystallography analysis of racemic **10d** and **12d** (Figure S5 and CCDC 2082689 and 2082690, respectively). The UV−vis absorption spectra of **10a−c**, **10e**, **12a−c**, and **12e** in chloroform are shown in Figure 1. Compared with pristine PDI, the *C*-shaped and *S*-shaped molecules fused with same heteroaromatics display similar bathochromic shifts due to the extension of π-conjugation. In contrast, fusions with different heterocycles have drastic effect on the absorption spectra.[15] The maximum

https://doi.org/10.1021/acs.orglett.2c00928
Org. Lett. 2022, 24, 3179−3183

Scheme 4. Modular Synthesis of *C*-Shaped PDI Heterohelicenes 10a−e and *S*-Shaped 12a−e

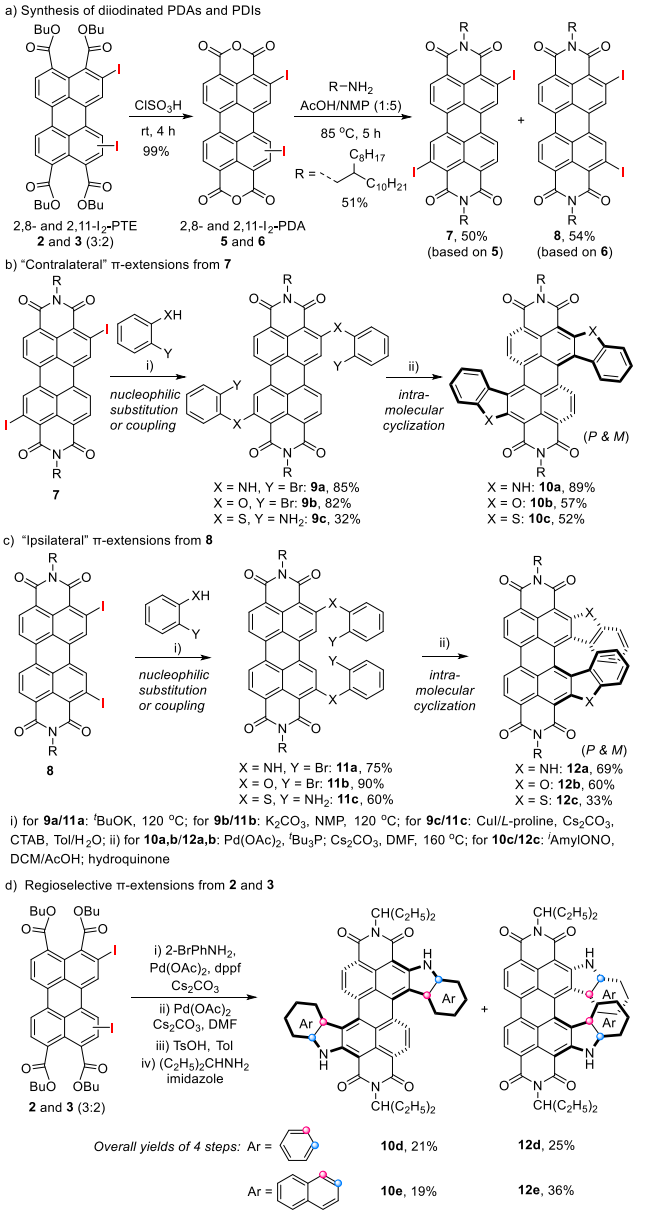

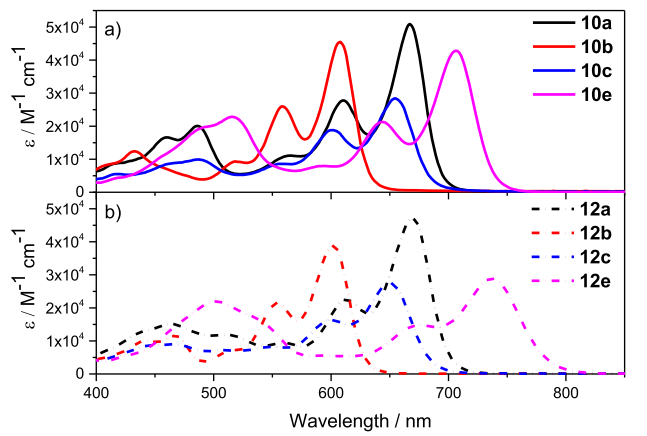

Figure 1. UV−vis absorption spectra of (a) **10a−c** and **10e** and (b) **12a−c** and **12e** (10 μM in chloroform, 298 K).

absorption peaks for **10e** (X = NH), **10a** (X = NH), **10c** (X = S), and **10b** (X = O) are 706, 666, 654, and 607 nm, respectively. The electrochemical behaviors of these PDI heterohelicenes were also compared using cyclic voltammetry (Figure S6 and Table S3). The distinct orientations of the two fused heteroaromatics in the *C*- and *S*-shaped molecules have only tiny effects on their redox potentials, whereas the incorporation of different heteroatoms can finely tune the energy levels as a result of different electron-donating properties of the N, S, and O atoms.

Through chiral high-performance liquid chromatography (HPLC), enantiomers (*P* or *M*) of *C*-shaped PDI-azahelicenes **12a**, **12d**, and **12e** were separated from each other. When the diphenyl ether solution of **12a**-*P* was heated at 523 K for 30 min and monitored by circular dichroism (CD) spectroscopy, isomerization was not observed (Figure S8), indicating the compound's conformational stability.[16] The dissymmetry factors of these *C*-shaped skeletons achieved about half the value of PDI double helicene **I**.[7] In contrast, enantiomers of *S*-shaped PDI heterohelicenes **10a−c** were not separated due to the much lower energy barriers of racemization.[17] The stacking behavior of **12a**-*P* and **12d**-*P* with different imide substituents was then studied using UV−vis spectroscopy. In temperature-dependent UV−vis spectra of **12a**-*P* recorded in apolar methylcyclohexane (MCH), the continuous small red-shift of the absorption edge and the drastically decreased A_{0-0}/A_{0-1} ratio upon cooling suggest the formation of PDI aggregates. The solid-state absorption spectra of **12a**-*P* and **12d**-*P* have bandwidths and intensities similar to those in the spectrum of **12a**-*P* (2 mM) in MCH at 283 K (Figure S11), indicating their identical aggregation modes in both solution and the solid state. Fortunately, single crystals of **12d**-*P* and **12d**-*M* were both obtained by the slow diffusion of MeCN into their dichloromethane solutions, and the solid-state structures were elucidated by single-crystal X-ray diffraction (Figure 2 and CCDC 2088594 and 2088593, respectively). The remarkable solid-state packing of enantiomerically pure **12d** features a spiral-stair like superhelix structure. One helical turn is formed by eight molecules and has a pitch of 2.0 nm. The position and direction of each molecule gradually rotate around one axis. All molecules direct the unsubstituted side of the PDI core to the inner space of the helix and spread two indole rings to the exterior (Figure 2a and b). To avoid steric repulsion, each molecule needs to be slipped with each other, keeping the π-stacking between PDI cores and the $\pi-\pi$ overlap between outward neighboring indole rings (Figure 2c). In addition, the distribution of the dipole moments in a single column viewed along the top of the column highlights that the dipoles cancel within a helical pitch (Figure 2d).[18]

In conclusion, we have designed and synthesized two novel classes of PDI heterohelicenes using regioselective "contralateral" and "ipsilateral" π-extension routes based on efficient and selective Rh(III)-catalyzed 2,8- and 2,11-diiodinations of PTE. The variation in the relative strengths of the donor moieties (heteroaromatics) allowed the fine-tuning of the physicochemical properties depending on the need. As large asymmetric fused D−A systems, these helical π-systems exhibit strong dipole−dipole interactions as well as $\pi-\pi$ stacking interactions, suggesting their advanced applications in optoelectronic devices. The precise determination of the interactions between twisted helicenes would help to investigate the stacking structures directly and inspire the future development of 1D

https://doi.org/10.1021/acs.orglett.2c00928
Org. Lett. 2022, 24, 3179−3183

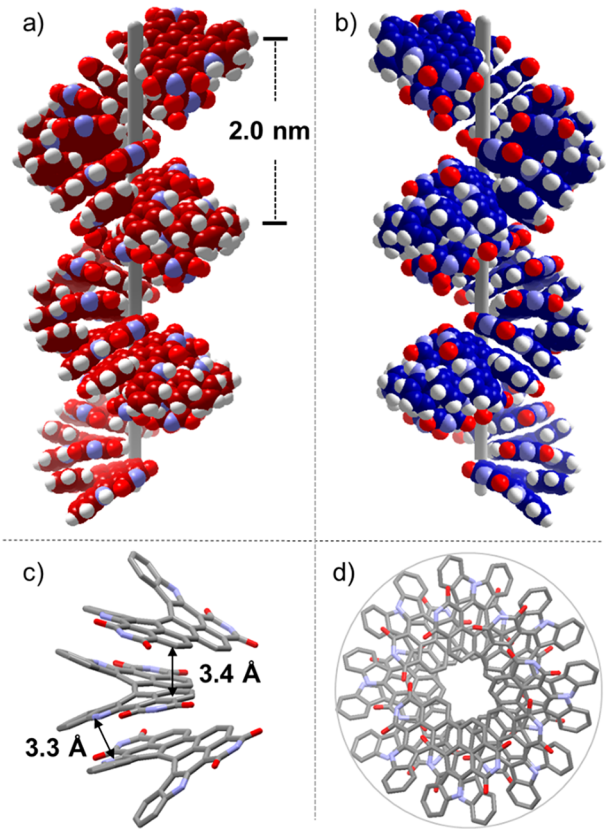

Figure 2. (a and b) Space-filling models of the helical π-stacking arrangements of enantiomerically pure **12d**-*P* and **12d**-*M*, respectively. *P*-Helical turns are shown in red, and *M*-helical turns are shown in blue. (c) Front view of π-stacks of **12d**-*P* with distances between the centroids of terminal indole or phenyl rings. (d) Top view of a single turn in the helical superstructure of **12d**-*P*. Hydrogen atoms in panels c and d and alkyl chains in panels a–d were omitted for clarity.

helical superstructures based on multifunctional π-skeletons with even larger steric hindrance or charge repulsion.

■ ASSOCIATED CONTENT

Supporting Information

The Supporting Information is available free of charge at https://pubs.acs.org/doi/10.1021/acs.orglett.2c00928.

General procedures, characterization data, CV curves, CD spectra, absorption and fluorescence spectra, and NMR spectra (PDF)

Accession Codes

CCDC 2082689–2082691 and 2088593–2088594 contain the supplementary crystallographic data for this paper. These data can be obtained free of charge via www.ccdc.cam.ac.uk/data_request/cif, or by emailing data_request@ccdc.cam.ac.uk, or by contacting The Cambridge Crystallographic Data Centre, 12 Union Road, Cambridge CB2 1EZ, UK; fax: +44 1223 336033.

■ AUTHOR INFORMATION

Corresponding Author

Jianbin Lin − *Department of Chemistry, College of Chemistry and Chemical Engineering, MOE Key Laboratory of Spectrochemical Analysis and Instrumentation, Xiamen University, Xiamen, Fujian 361005, P. R. China;* orcid.org/0000-0002-0064-3079; Email: jb.lin@xmu.edu.cn

Authors

Li Zhang − *Department of Chemistry, College of Chemistry and Chemical Engineering, MOE Key Laboratory of Spectrochemical Analysis and Instrumentation, Xiamen University, Xiamen, Fujian 361005, P. R. China*

Shuqi Chen − *Department of Chemistry, College of Chemistry and Chemical Engineering, MOE Key Laboratory of Spectrochemical Analysis and Instrumentation, Xiamen University, Xiamen, Fujian 361005, P. R. China*

Jianbao Jiang − *Department of Chemistry, College of Chemistry and Chemical Engineering, MOE Key Laboratory of Spectrochemical Analysis and Instrumentation, Xiamen University, Xiamen, Fujian 361005, P. R. China*

Xue Dong − *Department of Chemistry, College of Chemistry and Chemical Engineering, MOE Key Laboratory of Spectrochemical Analysis and Instrumentation, Xiamen University, Xiamen, Fujian 361005, P. R. China*

Yapeng Cai − *Department of Chemistry, College of Chemistry and Chemical Engineering, MOE Key Laboratory of Spectrochemical Analysis and Instrumentation, Xiamen University, Xiamen, Fujian 361005, P. R. China*

Hui-Jun Zhang − *Department of Chemistry, College of Chemistry and Chemical Engineering, MOE Key Laboratory of Spectrochemical Analysis and Instrumentation, Xiamen University, Xiamen, Fujian 361005, P. R. China;* orcid.org/0000-0001-9567-3010

Yun-Bao Jiang − *Department of Chemistry, College of Chemistry and Chemical Engineering, MOE Key Laboratory of Spectrochemical Analysis and Instrumentation, Xiamen University, Xiamen, Fujian 361005, P. R. China;* orcid.org/0000-0001-6912-8721

Complete contact information is available at: https://pubs.acs.org/10.1021/acs.orglett.2c00928

Notes

The authors declare no competing financial interest.

■ ACKNOWLEDGMENTS

We are grateful for financial support from the Natural Science Foundation of China (nos. 22071208 and 22171237) and the Youth Innovation Foundation of Xiamen (no. 3502Z20206058).

■ DEDICATION

This paper is dedicated to Prof. Pierre H. Dixneuf (Université de Rennes 1) for his outstanding contribution to catalysis.

■ REFERENCES

(1) (a) Shen, Y.; Chen, C.-F. Helicenes: Synthesis and Applications. *Chem. Rev.* **2012**, *112* (3), 1463–1535. (b) Mori, T. Chiroptical Properties of Symmetric Double, Triple, and Multiple Helicenes. *Chem. Rev.* **2021**, *121* (4), 2373–2412. (c) Schmidt, J. A.; Weatherby, J. A.; Sugden, I. J.; Santana-Bonilla, A.; Salerno, F.; Fuchter, M. J.; Johnson, E. R.; Nelson, J.; Jelfs, K. E. Computational Screening of Chiral Organic Semiconductors: Exploring Side-Group Functionalization and Assembly to Optimize Charge Transport. *Cryst. Growth Des.* **2021**, *21* (9), 5036–5049. (d) Dhbaibi, K.; Favereau, L.; Crassous, J. Enantioenriched Helicenes and Helicenoids Containing Main-Group Elements (B, Si, N, P). *Chem. Rev.* **2019**, *119* (14), 8846–8953. (e) Saal, F.; Zhang, F.; Holzapfel, M.; Stolte, M.; Michail, E.; Moos,

M.; Schmiedel, A.; Krause, A.-M.; Lambert, C.; Würthner, F.; Ravat, P. [n]Helicene Diimides (n = 5, 6, and 7): Through-Bond versus Through-Space Conjugation. *J. Am. Chem. Soc.* **2020**, *142* (51), 21298−21303. (f) Ravat, P.; Saal, F. Imide-Functionalized Helical PAHs: A Step towards New Chiral Functional Materials. *Synlett* **2021**, *32* (19), 1879−1890.

(2) (a) Chen, S.; Slattum, P.; Wang, C.; Zang, L. Self-Assembly of Perylene Imide Molecules into 1D Nanostructures: Methods, Morphologies, and Applications. *Chem. Rev.* **2015**, *115* (21), 11967−98. (b) Wöhrle, T.; Wurzbach, I.; Kirres, J.; Kostidou, A.; Kapernaum, N.; Litterscheidt, J.; Haenle, J. C.; Staffeld, P.; Baro, A.; Giesselmann, F.; Laschat, S. Discotic Liquid Crystals. *Chem. Rev.* **2016**, *116* (3), 1139−1241.

(3) (a) Nakano, K.; Oyama, H.; Nishimura, Y.; Nakasako, S.; Nozaki, K. λ5-Phospha[7]helicenes: Synthesis, Properties, and Columnar Aggregation with One-Way Chirality. *Angew. Chem., Int. Ed.* **2012**, *51* (3), 695−699. (b) Zeng, C.; Xiao, C.; Feng, X.; Zhang, L.; Jiang, W.; Wang, Z. Electron-Transporting Bis(heterotetracenes) with Tunable Helical Packing. *Angew. Chem., Int. Ed.* **2018**, *57* (34), 10933−10937. (c) Xiao, X.; Pedersen, S. K.; Aranda, D.; Yang, J.; Wiscons, R. A.; Pittelkow, M.; Steigerwald, M. L.; Santoro, F.; Schuster, N. J.; Nuckolls, C. Chirality Amplified: Long, Discrete Helicene Nanoribbons. *J. Am. Chem. Soc.* **2021**, *143* (2), 983−991.

(4) (a) Hatakeyama, T.; Hashimoto, S.; Oba, T.; Nakamura, M. Azaboradibenzo[6]helicene: Carrier Inversion Induced by Helical Homochirality. *J. Am. Chem. Soc.* **2012**, *134* (48), 19600−19603. (b) Yang, Y.; da Costa, R. C.; Fuchter, M. J.; Campbell, A. J. Circularly polarized light detection by a chiral organic semiconductor transistor. *Nat. Photonics* **2013**, *7* (8), 634−638. (c) Yang, Y.; Rice, B.; Shi, X.; Brandt, J. R.; Correa da Costa, R.; Hedley, G. J.; Smilgies, D. M.; Frost, J. M.; Samuel, I. D. W.; Otero-de-la-Roza, A.; Johnson, E. R.; Jelfs, K. E.; Nelson, J.; Campbell, A. J.; Fuchter, M. J. Emergent Properties of an Organic Semiconductor Driven by its Molecular Chirality. *ACS Nano* **2017**, *11* (8), 8329−8338.

(5) Ghosh, S.; Li, X.-Q.; Stepanenko, V.; Würthner, F. Control of H- and J-Type π Stacking by Peripheral Alkyl Chains and Self-Sorting Phenomena in Perylene Bisimide Homo- and Heteroaggregates. *Chem. Eur. J.* **2008**, *14* (36), 11343−11357.

(6) Echue, G.; Lloyd-Jones, G. C.; Faul, C. F. J. Chiral Perylene Diimides: Building Blocks for Ionic Self-Assembly. *Chem. Eur. J.* **2015**, *21* (13), 5118−5128.

(7) Zhang, L.; Song, I.; Ahn, J.; Han, M.; Linares, M.; Surin, M.; Zhang, H.-J.; Oh, J. H.; Lin, J. π-Extended Perylene Diimide Double-heterohelicenes as Ambipolar Organic Semiconductors for Broadband Circularly Polarized Light Detection. *Nat. Commun.* **2021**, *12* (1), 142.

(8) Yue, W.; Jiang, W.; Böckmann, M.; Doltsinis, N. L.; Wang, Z. Regioselective Functionalization of Core-Persubstituted Perylene Diimides. *Chem. Eur. J.* **2014**, *20* (18), 5209−5213.

(9) (a) Li, Y.; Gao, J.; Di Motta, S.; Negri, F.; Wang, Z. Tri-N-annulated hexarylene: an approach to well-defined graphene nanoribbons with large dipoles. *J. Am. Chem. Soc.* **2010**, *132* (12), 4208−4213. (b) Ueda, M.; Aoki, T.; Akiyama, T.; Nakamuro, T.; Yamashita, K.; Yanagisawa, H.; Nureki, O.; Kikkawa, M.; Nakamura, E.; Aida, T.; Itoh, Y. Alternating Heterochiral Supramolecular Copolymerization. *J. Am. Chem. Soc.* **2021**, *143* (13), 5121−5126. (c) Würthner, F. Dipole-Dipole Interaction Driven Self-Assembly of Merocyanine Dyes: From Dimers to Nanoscale Objects and Supramolecular Materials. *Acc. Chem. Res.* **2016**, *49* (5), 868−76.

(10) Wu, J.; He, D.; Zhang, L.; Liu, Y.; Mo, X.; Lin, J.; Zhang, H. J. Direct Synthesis of Large-Scale Ortho-Iodinated Perylene Diimides: Key Precursors for Functional Dyes. *Org. Lett.* **2017**, *19* (19), 5438−5441.

(11) (a) Würthner, F.; Stepanenko, V.; Chen, Z.; Saha-Möller, C. R.; Kocher, N.; Stalke, D. Preparation and Characterization of Regioisomerically Pure 1,7-Disubstituted Perylene Bisimide Dyes. *J. Org. Chem.* **2004**, *69* (23), 7933−7939. (b) Yuan, Z.; Li, J.; Xiao, Y.; Li, Z.; Qian, X. Core-Perfluoroalkylated Perylene Diimides and Naphthalene Diimides: Versatile Synthesis, Solubility, Electrochemistry, and Optical Properties. *J. Org. Chem.* **2010**, *75* (9), 3007−3016. (c) Guo, Y.; Li, Y.; Awartani, O.; Zhao, J.; Han, H.; Ade, H.; Zhao, D.; Yan, H. A Vinylene-Bridged Perylenediimide-Based Polymeric Acceptor Enabling Efficient All-Polymer Solar Cells Processed under Ambient Conditions. *Adv. Mater.* **2016**, *28* (38), 8483−8489. (d) Zeng, C.; Meng, D.; Jiang, W.; Wang, Z. Synthesis of Isomeric Perylenodithiophene Diimides. *Org. Lett.* **2018**, *20* (20), 6606−6609.

(12) (a) Teraoka, T.; Hiroto, S.; Shinokubo, H. Iridium-Catalyzed Direct Tetraborylation of Perylene Bisimides. *Org. Lett.* **2011**, *13* (10), 2532−2535. (b) Battagliarin, G.; Li, C.; Enkelmann, V.; Müllen, K. 2,5,8,11-Tetraboronic ester perylenediimides: a next generation building block for dye-stuff synthesis. *Org. Lett.* **2011**, *13* (12), 3012−5.

(13) Tóth, B. L.; Monory, A.; Egyed, O.; Domján, A.; Bényei, A.; Szathury, B.; Novák, Z.; Stirling, A. The ortho effect in directed C−H activation. *Chem. Sci.* **2021**, *12* (14), 5152−5163.

(14) (a) Sambiagio, C.; Schönbauer, D.; Blieck, R.; Dao-Huy, T.; Pototschnig, G.; Schaaf, P.; Wiesinger, T.; Zia, M. F.; Wencel-Delord, J.; Besset, T.; Maes, B. U. W.; Schnürch, M. A comprehensive overview of directing groups applied in metal-catalysed C−H functionalisation chemistry. *Chem. Soc. Rev.* **2018**, *47* (17), 6603−6743. (b) Tomberg, A.; Muratore, M. É.; Johansson, M. J.; Terstiege, I.; Sköld, C.; Norrby, P.-O. Relative Strength of Common Directing Groups in Palladium-Catalyzed Aromatic C-H Activation. *iScience* **2019**, *20*, 373−391.

(15) Stepien, M.; Gonka, E.; Zyla, M.; Sprutta, N. Heterocyclic Nanographenes and Other Polycyclic Heteroaromatic Compounds: Synthetic Routes, Properties, and Applications. *Chem. Rev.* **2017**, *117* (4), 3479−3716.

(16) Ravat, P. Carbo[*n*]helicenes Restricted to Enantiomerize: An Insight into the Design Process of Configurationally Stable Functional Chiral PAHs. *Chem. Eur. J.* **2021**, *27* (12), 3957−3967.

(17) **10e** could also be separated using chiral HPLC but was found to racemize very slowly (see Figure S10).

(18) Watanabe, G.; Watanabe, H.; Suzuki, K.; Yuge, H.; Yoshida, S.; Mandai, T.; Yoneda, S.; Sato, H.; Hara, M.; Yoshida, J. Visualizing the helical stacking of octahedral metallomesogens with a chiral core. *Chem. Commun.* **2020**, *56* (81), 12134−12137.

https://doi.org/10.1021/acs.orglett.2c00928
Org. Lett. 2022, 24, 3179−3183